The following resources related to this article are available online at
www.sciencemag.org (this information is current as of November 24, 2006):

Updated information and services, including high-resolution figures, can be found in the online
version of this article at:
http://www.sciencemag.org/cgi/content/full/314/5803/1283

Supporting Online Material can be found at:
http://www.sciencemag.org/cgi/content/full/314/5803/1283/DC1

This article **cites 19 articles**, 2 of which can be accessed for free:
http://www.sciencemag.org/cgi/content/full/314/5803/1283#otherarticles

This article appears in the following **subject collections**:
Atmospheric Science
http://www.sciencemag.org/cgi/collection/atmos

Information about obtaining **reprints** of this article or about obtaining **permission to reproduce**
this article in whole or in part can be found at:
http://www.sciencemag.org/help/about/permissions.dtl

period in less than a million years would require a YORP acceleration rate a factor of five times as high as at present, which is plausible if Alpha's initial mass distribution were less symmetric than it is now. Once Beta formed, continued rotational acceleration of Alpha would be regulated as described previously, the resurfacing making the system more symmetric and diminishing YORP's effectiveness over time.

Could KW4 have formed in the main asteroid belt and subsequently migrated into an Earth-crosser? Recent discoveries reveal a substantial population of small, inner main-belt binaries with characteristics similar to near-Earth binaries (*33*). Collisions and YORP can form binaries within the main belt, but formation by tidal flybys is extremely unlikely. If KW4 formed in the main belt, then its age must be on the order of 10^8 years and it must have survived multiple close-Earth approaches (*3*) that could have strongly excited it while avoiding any that could disrupt it. Thus, formation of KW4 in a near-Earth orbit through some combination of tidal and YORP torques seems more likely.

References and Notes

1. J. L. Margot *et al.*, *Science* **296**, 1445 (2002).
2. H. Kinoshita, *Publ. Astron. Soc. Jpn.* **24**, 423 (1972).
3. S. J. Ostro *et al.*, *Science* **314**, 1276 (2006); published online 12 October 2006, 10.1126/science.1133622.
4. A. J. Maciejewski, *Celestial Mech. Dyn. Astron.* **63**, 1 (1995).
5. R. A. Werner, D. J. Scheeres, *Celestial Mech. Dyn. Astron.* **91**, 337 (2005).
6. E. G. Fahnestock, D. J. Scheeres, *Celestial Mech. Dyn. Astron.*, in press.
7. This polyhedral formulation reduces the mutual potential to a series of joint summations over the facets of each model, 9108 for Alpha and 2292 for Beta. The number of operations for each evaluation of the mutual potential, force, and moment is on the order of the product of those numbers, or 21 million.
8. T. Lee, M. Leok, N. H. McClamroch, available at http://arxiv.org/abs/math.NA/0508365
9. The complete equations of motion, model, and an animation are available as supporting material on *Science* Online.
10. Over time scales of 77,000 years, *N*-body gravitational perturbations cause KW4's argument of perihelion to circulate and its eccentricity, inclination, and perihelion distance to oscillate significantly, while its semimajor axis remains approximately constant as a result of a Kozai resonance (*34*). KW4's heliocentric eccentricity and perihelion vary between current values of $e = 0.68$ and $q = 0.20$ AU to $e = 0.81$ and $q = 0.12$ AU, and its heliocentric inclination varies from 39° (currently) to 14°.
11. P. Farinella, *Icarus* **96**, 284 (1992).
12. W. F. Bottke Jr., H. J. Melosh, *Icarus* **124**, 372 (1996).
13. J. A. Burns, V. S. Safronov, *Mon. Not. R. Astron. Soc.* **165**, 403 (1973).
14. G. Colombo, *Astron. J.* **71**, 891 (1966).
15. A more detailed description is provided in the supplemental material.
16. V. Guibout, D. J. Scheeres, *Celestial Mech. Dyn. Astron.* **87**, 263 (2003).
17. A. Fujiwara *et al.*, *Science* **312**, 1330 (2006).
18. D. J. Scheeres, Stability of Binary Asteroids Formed Through Fission [#1632], abstract presented at the 37th Lunar and Planetary Science Conference (2006).
19. C. D. Murray, S. F. Dermott, *Solar System Dynamics* (Cambridge Univ. Press, Cambridge, 1999), pp. 160–174.
20. Typical values for rocky bodies are $\mu_{rock} = 5 \times 10^{10}$ Nm^{-2} and $Q = 100$.
21. H. He, T. J. Ahrens, *Int. J. Rock Mech. Min. Sci. Geomech.* **31**, 525 (1994).
22. The supporting material provides additional details on this calculation.
23. D. P. Rubincam, *Icarus* **148**, 2 (2000).
24. The effect of solar radiation forces on Beta may also influence orbital evolution via the Binary YORP effect (*35*). Applying the theory in (*35*) to the KW4 system predicts that the orbit is shrinking at a rate of 0.8 m per year. Such rapid collapse seems inconsistent with the existence of the system unless it formed very recently.
25. The YORP rotational acceleration is found by applying Rubincam's method (*24*) to the Alpha model and averaging over one heliocentric orbit period.
26. D. J. Scheeres, J. Bellerose, *Dyn. Syst. Int. J.* **20**, 23 (2005).
27. J. K. Miller *et al.*, *Icarus* **155**, 3 (2002).
28. K. J. Walsh, D. C. Richardson, *Icarus* **180**, 201 (2006).
29. D. C. Richardson, K. J. Walsh, *Annu. Rev. Earth Planet. Sci.* **34**, 47 (2006).
30. F. Roig, R. Duffard, P. Penteado, D. Lazzaro, T. Kodama, *Icarus* **165**, 355 (2003).
31. D. G. Korycansky, *Astrophys. Space Sci.* **291**, 57 (2004).
32. W. F. Bottke Jr., D. Vokrouhlický, D. P. Rubincam, M. Broz, *Asteroids III*, Bottke *et al.*, Eds. (Univ. Arizona Press, Tucson, 2002), p. 405.
33. P. Pravec *et al.*, *Icarus* **181**, 63 (2006).
34. G. F. Gronchi 2006. NEODys Web site. http://newton.dm.unipi.it/cgi-bin/neodys/neoibo?objects:1999KW4;main.
35. M. Ćuk, J. A. Burns, *Icarus* **176**, 418 (2005).
36. Research at the University of Michigan was supported by NASA's Planetary Geology and Geophysics Program, by the Jet Propulsion Laboratory (JPL) California Institute of Technology (Caltech) Director's Research and Development Fund, and by the Air Force Office of Scientific Research. Some of this work was performed at JPL Caltech under contract with NASA. The supercomputers used in this investigation were provided by funding from JPL Institutional Computing and Information Services and NASA Directorates of Aeronautics Research, Science, Exploration Systems, and Space Operations. This material is based in part on work supported by NASA under the Science Mission Directorate Research and Analysis Programs. C.M. was partially supported by NSF grant AST-0205975. J.L.M. was supported in part by NASA grant NNG04GN31G. P.P. and P.S. were supported by the Grant Agency of the Czech Republic, Grant 205/05/0604.

Ongoing Buildup of Refractory Organic Carbon in Boreal Soils During the Holocene

R. H. Smittenberg,[1]* T. I. Eglinton,[2] S. Schouten,[1] J. S. Sinninghe Damsté[1]

Radiocarbon ages of vascular plant wax–derived *n*-alkanes preserved in well-dated Holocene sediments in an anoxic fjord (Saanich Inlet, Canada) were found to be not only substantially older than the depositional age but increasingly so during the Holocene. Assuming that *n*-alkanes serve as a proxy for recalcitrant terrigenous organic matter, this indicates that the accumulation of refractory organic carbon in soils that developed after the deglaciation of the American Pacific Northwest is ongoing and may still be far from equilibrium with mineralization and erosion rates.

Estimated at ~1500 Pg, soil organic carbon (SOC) constitutes the largest active OC pool on the globe (*1, 2*), and consequently the fluxes of OC to and from this reservoir are important for the carbon budgets in the bio- and geosphere (*1, 3*). Refractory organic matter makes up approximately half of the SOC pool because of its resistance to degradation (*4*), and it is this pool that is ultimately responsible for long-term terrestrial carbon storage (*1, 5*). However, our understanding of the long-term buildup of SOC is largely derived from studies of present-day soils, and there is a paucity of temporal records of SOC dynamics. Because of its complex and heterogeneous nature, the accumulation, erosion, and especially mineralization rates of refractory SOC are hard to determine, which hinders modeling of fluxes to and from this carbon pool (*1, 3, 4, 6*). For instance, the extent to which the higher-latitude soils and peats have been, or still are, expanding and/or changing in composition after their initial buildup after the most recent deglaciation remains an open question (*1, 3, 5, 6*). Data to substantiate hypotheses about the global carbon cycle over millennial time scales are very limited, and for the terrigenous component of this cycle, depend mainly on soil chronosequences (*7, 8*); mass balance studies of various SOC pools, aided by radiocarbon analysis (*6*); vegetation reconstructions coupled with soil carbon content (*9*); and models (*4*). A limiting factor in these studies is that they rely on inventories of biomass and active soil, whose properties have probably changed over time.

Coastal and lake sediments contain a temporal record of soil organic matter delivered from adjacent watersheds, and these records may

[1]Department of Marine Biogeochemistry and Toxicology, Royal Netherlands Institute of Sea Research, Post Office Box 59, 1790 AB, Den Burg, Netherlands. [2]Department of Marine Chemistry and Geochemistry, Woods Hole Oceanographic Institution, Woods Hole, MA 02543, USA.

*To whom correspondence should be addressed. Present address: School of Oceanography, University of Washington, Box 355351, Seattle, WA 98195, USA. E-mail: smitten@u.washington.edu

provide insight into past changes in the refractory SOC pool. We examined sediments of Saanich Inlet, Canada (10), which contain a high-temporal-resolution record spanning the late Holocene, lying above a less-well-resolved early Holocene sequence and late Pleistocene glaciomarine deposits. Because of high sediment accumulation rates (11) and permanent anoxic bottom-water conditions, the sedimentary organic matter and the sediment structure have been well preserved (10, 12), enabling annual dating of the core back to ~6000 years before the present (yr B.P.) by means of varve counting (13). We analyzed the distribution, stable carbon isotopic composition, and radiocarbon composition of vascular plant–derived long-chain n-alkanes from seven well-dated laminated sediment layers ranging from recent to 5500 yr B.P. (14), as well as layers just below the well-dated section and a late Pleistocene layer (Table 1). Both the stable carbon isotopic ($\delta^{13}C$) compositions (table S1) and the distribution of the n-alkanes (Fig. 1), as reflected in the carbon preference index (CPI) (Table 1), suggest that they are predominantly derived from C_3 vascular plant material, admixed with

some fossil alkanes of petrogenic origin, such as from weathering of sedimentary rocks (14, 15). This is in agreement with earlier observations in the Fraser River basin (16) near Saanich Inlet. There is a preponderance of evidence that long-chain n-alkanes are resistant to degradation (17, 18), and previous studies indicate that they can serve as a proxy for the refractory SOC pool (19, 20). The reasons for their recalcitrance, and that of the majority of SOC, may be that they are intimately associated with the mineral fraction (2, 3, 21, 22). The specific surface area of minerals appears to play an important role in OC preservation, with adsorption providing some sort of physical protection against water-soluble microbial enzymes. Such protection may also be provided by the hydrophobic nature of (humified) organic matter or by micropores within soil aggregates (3). Low temperatures and low-oxygen conditions related to waterlogging also decrease OC degradation (3).

The major sources of terrigenous sediment that enters Saanich Inlet are the nearby Cowichan River and the large Fraser River across the Strait of Georgia; this sediment is augmented by material discharged from local streams (11).

Soils in the watersheds of these rivers should thus be the main source of the terrigenous OC, and thereby n-alkanes, in the Saanich Inlet sediments (19). Erosion of the land surface in British Columbia has continued unabated since the last deglaciation, with a dominance of secondary remobilization of Quaternary sediments over primary denudation (23). Because of high flows during the spring freshets and the high topographic relief of the region, most of the fine-grained sediment (silt and clay), and thereby the bulk of eroded SOC (2), experience a relatively short residence time within the river systems (24). Intermediate reservoirs that would delay incorporation of the soil carbon signal into the marine sedimentary record are therefore of limited importance. Besides being derived from soil organic matter, sedimentary n-alkanes may also be derived directly from living vegetation, typically transported by wind after ablation of the leaf waxes (25). Substantial amounts of contemporary n-alkanes from fresh vegetation would result in distinctly higher radiocarbon contents of the odd–carbon-numbered C_{27}-C_{31} n-alkanes deposited after aboveground nuclear weapons testing as compared to "pre-bomb" material. This is not the case (Table 1), which suggests that a direct input from vegetation plays a minor role.

When the calibrated ages of the odd C_{27}-C_{31} n-alkanes are compared with the varve ages of the laminated sediments, it is immediately apparent that there is a discrepancy between these two ages and that this discrepancy increases toward the present (Fig. 2). Such a trend was not observed in marine-derived biomarkers in the same setting (26), indicating that this is clearly a different, exclusively terrigenous signal. For the laminated section, linear regression between the sediment age and the sediment–n-alkane age offset yields a squared correlation coefficient (R^2) of 0.68. The outlier at ~500 yr B.P. may reflect heterogeneities in the nature of the eroded material: Possibly this sample contained an anomalously large fraction of fresh vascular plant detritus. When this outlier is excluded, the R^2 increases to 0.98. Three properties of the

Fig. 1. Measured and modeled distribution and $\delta^{13}C$ values of the n-alkane fraction from the sediment interval corresponding to 2533 to 2702 yr B.P. as a representative of the studied samples. Numbers beginning with n refer to carbon chain length. The modeled data represent the outcome of a mixing model with a fossil (10%) and contemporary vascular plant source (90%) with estimated $\delta^{13}C$ and CPI end-member values (14). Because the model is a simplification of reality, a perfect fit cannot be reached with just two end-members. However, the proportions used give a reasonable estimate. ‰, per mil.
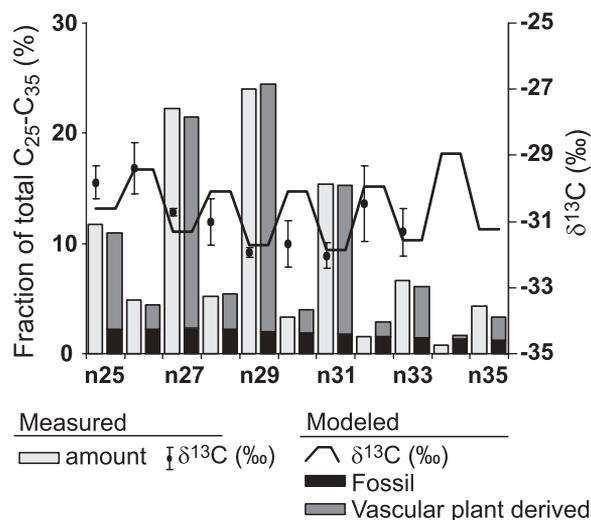

Table 1. Radiocarbon content, calibrated age, and other properties of sedimentary n-alkanes (odd C_{27-31}). cal, calendar.

Sediment age (varve-based) (18)	n-Alkanes $\Delta^{14}C$ (± 8‰)	Calibrated age (cal yr B.P.)*	Concentration (µg/g dry sediment)	CPI†	Fossil fraction (±5%)‡
1984–1998 A.D.	−458	5473 (5599) 5730	4.4	2.7	25
1932–1950 A.D.	−464	5606 (5657) 5844	3.1	4.1	10
568–465 B.P.	−417	4828 (4854) 4893	2.8	4.3	10
1111–977 B.P.	−498	6234 (6290) 6354	2.1	4.9	10
2330–2520 B.P.	−538 ± 40	6666 (6997) 7388	2.2	4.7	10
2707–2533 B.P.	−546	7131 (7215) 7285	1.8	4.8	10
3600–3500 B.P.	−	−	1.8	4.1	10
4940–4840 B.P.	−626	8476 (8617) 8948	0.8	4.8	10
6300–6500 B.P.§	−701 ± 95	10132 (11120) 12339	2.2	4.0	15
11500–13000 B.P.‖	−806 ± 41	15256 (15724) 16374	1.6	4.0	15

*The calibrated age ranges are 1σ confidence intervals. The age in parentheses has the highest probability.   †CPI = 0.5 ×[(C_{25} + C_{27} + C_{29} + C_{31}) + (C_{27} + C_{29} + C_{31}+ C_{33})]/(C_{26} + C_{28} + C_{30} + C_{32}). The average chain length for C_{25}-C_{35} is 28.8 ± 0.3 for all samples.   ‡Estimates based on two end-member models (14).   §Sample from intermittently laminated section. Age was extrapolated using the sedimentation rate of varve-counted sediment above (13).   ‖Glaciomarine silty clay deposited during late deglaciation. The minimum age is based on radiocarbon-dated above-lying sediment (13) and the maximum age on the timing of glacial retreat (27).

regression line are notable: (i) the correlation is linear; (ii) the calculated intercept age (that is, *n*-alkane age = calendar age) is similar to the time of deglaciation of the area, between 14,000 and 11,500 yr B.P. (27); and (iii) the age offset of 5500 years in the youngest sediments represents about half of the Holocene time span.

The CPI, in conjunction with the $\delta^{13}C$ values of the individual *n*-alkanes, can be used to estimate the relative contribution of fossil (radiocarbon-dead) and Holocene-aged soil *n*-alkanes (14, 28) (Table 1 and supporting online text). Recalibration to calendar ages after correction of the *n*-alkane $\Delta^{14}C$ value for fossil inputs produces Holocene-sourced *n*-alkane ages (Fig. 2). The intercept of the regression line comes closer toward the real onset of the Holocene at 11,500 yr B.P. (27). At that time, the entire region became vegetated, although plants had already established themselves in the lowlands of the area as early as 13,500 yr B.P., as evidenced from radiocarbon-dated wood fragments in the Fraser moraines (27). The fossil-corrected *n*-alkane ages from the older nonlaminated sediments are in agreement with our interpretation. However, uncertainties in dating the *n*-alkanes and the sediments, together with uncertainties in fossil alkane estimates, make an interpretation of these data tentative, and we therefore refrain from drawing any further inferences from them.

The average age offset of the odd $C_{27}-C_{31}$ *n*-alkanes of the pre-bomb sediment after a correction for 10% fossil alkanes is ~4700 years (Fig. 2), whereas an equal contribution of *n*-alkanes aged from 0 to 11,000 yr B.P. would have resulted in an average age offset of 5500 years. This bias toward younger *n*-alkane ages

suggests that, as expected, some loss of refractory soil carbon by either mineralization or erosion must have occurred, although it is equally feasible that younger topsoils are preferentially eroded as compared to older and more deeply buried material. Regardless, it is evident that the average *n*-alkane ages have been increasing in a near-linear fashion toward the present, strongly suggesting that any loss due to erosion or mineralization is still largely outpaced by accumulation.

An alternative scenario that would produce the observed *n*-alkane age profile while allowing for substantially higher erosion and/or mineralization rates is one of continuously decreasing terrestrial primary productivity toward the present. In that case, the stock and concentration of *n*-alkanes in the drainage basin should diminish, whereas a more steady-state primary production and ongoing accumulation would be reflected by an increasing flux to the Saanich Inlet sediments toward the present. By using varve thickness data (13) in combination with wet bulk density and porosity data (10, 12, 13), we estimated the sediment accumulation rates (Fig. 3) in the laminated section. The accumulation rates of the odd $C_{27}-C_{31}$ *n*-alkanes to the sediment were then determined from their concentrations (Table 1). The fluxes of the Holocene-aged *n*-alkanes show an increasing trend toward the present, whereas this is not the case for the bulk sediment accumulation rate. This implies that the primary cause of the increasing odd $C_{27}-C_{31}$ *n*-alkane accumulation rate in the sediment must be a growing concentration of *n*-alkanes within the sediment load, which is consistent with a buildup of terrigenous

OC in the area. Postdepositional degradation of *n*-alkanes within the Saanich Inlet sediment does not appear to be an important factor (12, 17).

Although this study was done using long-chain *n*-alkanes only, the observed trends are probably valid for a larger range of refractory vascular plant–derived organic compounds (17, 18). These findings indicate that the refractory SOC pool of the Pacific Northwest is still increasing as a long-term response to the last deglaciation. Ongoing accumulation of refractory OC may be a broader phenomenon in boreal soils, or even in other biomes worldwide. However, similar studies to those undertaken here would be needed to verify this, because factors such as mineralogy, climate, and cultivation have an impact on the decomposition and preservation of all organic matter fractions, including the recalcitrant pool (3). Although our results appear to contradict some studies using natural ^{13}C labels (29) that find no evidence of a highly recalcitrant soil carbon pool, they corroborate other findings of old radiocarbon ages of refractory carbon fractions and *n*-alkanes in a large array of soils (4, 6, 20, 30, 31) and suggest that the turnover time of this carbon pool is 10,000 to 100,000 years or more and not 1000 to 10,000 years as is often used in soil carbon models (4). These findings challenge the notion that the current production of refractory organic matter is balanced by decomposition and erosion after a few thousand years, as inferred via

Fig. 2. Age offset between odd–carbon-numbered $C_{27}-C_{31}$ *n*-alkanes and sediments. Black diamonds represent offsets calculated with calibrated *n*-alkane ages given in Table 1. Error bars denote age uncertainty (1σ) after calibration. The data point at ~500 yr B.P. was not used for the regression line. Gray dots represent age offsets of Holocene-aged soil-derived *n*-alkanes with the sediments after correcting for the fossil fraction given in Table 1. The gray-shaded areas around the non-laminated fossil-corrected values represent their uncertainty based on the original ^{14}C value uncertainties and age constraints. Ka cal BP, thousands of calendar years before the present.
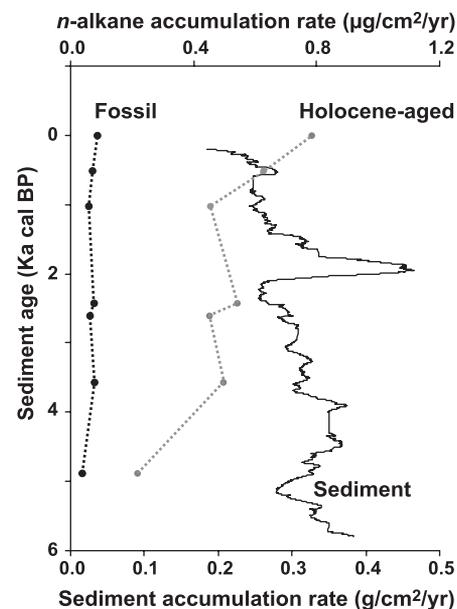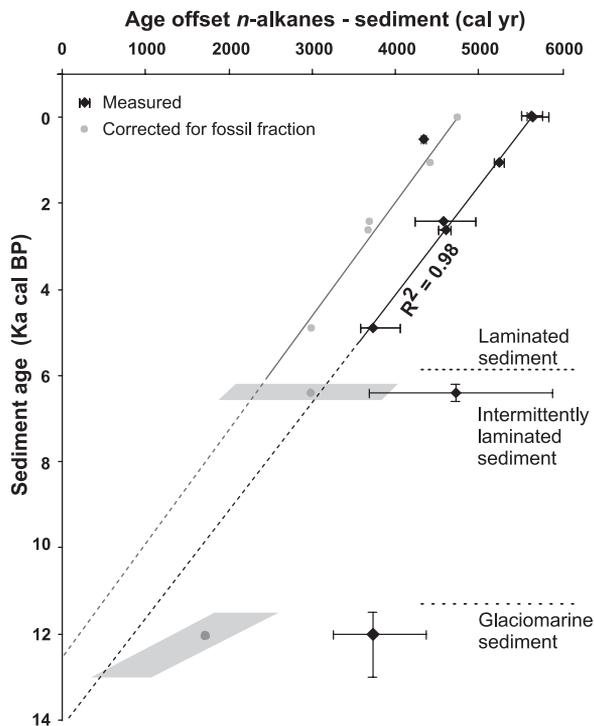

Fig. 3. *n*-Alkane and sediment accumulation rates of the laminated section of Saanich Inlet. Solid line, sediment; stippled black line, fossil *n*-alkanes; stippled gray line, Holocene (soil) *n*-alkanes. *n*-Alkane accumulation rates were calculated based on varve thickness (13), wet bulk density (10), and porosity data and modeling (10, 11, 13), together with the concentrations and estimated fossil fraction of the *n*-alkanes listed in Table 1.

chronosequences (*7*) or soil respiration measurements (*31*). The assumption that soils are in a steady state is also called into question, especially because it is recognized that refractory OC has been building up in soils exposed since the last glacial (*1*, *5*). This new paradigm likely has its main impact on carbon budget models that calculate sources, sinks, and fluxes within the global carbon cycle on longer time scales (>1000 years). This could be of relevance, for example, to studies that link vegetation type to soil carbon content in order to estimate changing carbon storage on land through time (*9*). It places the terrestrial biosphere in a more prominent position as a slow but progressively important atmospheric carbon sink on geologic time scales and may even influence current predictions about carbon cycling and soil carbon storage in response to elevated atmospheric CO_2 levels.

References and Notes

1. R. Amundson, *Annu. Rev. Earth Planet. Sci.* **29**, 535 (2001).
2. J. I. Hedges, R. G. Keil, *Mar. Chem.* **49**, 81 (1995).
3. E. A. Davidson, I. A. Janssens, *Nature* **440**, 165 (2006).
4. P. D. Falloon, P. Smith, *Biol. Fertil. Soils* **30**, 388 (2000).
5. J. W. Harden, E. T. Sundquist, R. F. Stallard, R. K. Mark, *Science* **258**, 1921 (1992).
6. E. A. Paul, H. P. Collins, S. W. Leavitt, *Geoderma* **104**, 239 (2001).
7. W. H. Schlesinger, *Nature* **348**, 232 (1990).
8. M. S. Torn *et al.*, *Nature* **389**, 170 (1997).
9. J. M. Adams, H. A. Faure, *Global Planet. Change* **16-17**, 3 (1998).
10. B. D. Bornhold *et al.*, *Proceedings of the Ocean Drilling Program, Initial Reports, 169S* (Ocean Drilling Program, College Station, TX, 1998), pp. 5–138.
11. S. M. Gucluer, M. G. Gross, *Limn. Oceanogr.* **9**, 359 (1964).
12. M. R. McQuoid, M. J. Whiticar, S. E. Elvert, T. F. Pederson, *Mar. Geol.* **174**, 273 (2001).
13. A. J. Nederbragt, J. W. Thurow, *Mar. Geol.* **174**, 95 (2001).
14. Materials and methods are available as supporting material on *Science* Online.
15. J. W. Collister, G. Rieley, B. Stern, G. Eglinton, B. Fry, *Org. Geochem.* **21**, 619 (1994).
16. M. B. Yunker, R. W. MacDonald, *Org. Geochem.* **34**, 1429 (2003).
17. F. S. Brown, M. J. Baedecker, A. Nissenbaum, I. R. Kaplan, *Geochim. Cosmochim. Acta* **36**, 1185 (1972).
18. M.-Y. Sun, S.-G. Wakeham, *Geochim. Cosmochim. Acta* **58**, 3395 (1994).
19. F. G. Prahl, G. J. De Lange, S. Scholten, G. L. Cowie, *Org. Geochem.* **27**, 141 (1997).
20. Y. Huang, *Soil Sci. Soc. Am. J.* **63**, 1181 (1999).
21. M. J. Kennedy, D. R. Pevear, R. J. Hill, *Science* **295**, 657 (2002).
22. L. M. Mayer, L. L. Schick, K. R. Hardy, R. Wagai, J. McCarthy, *Geochim. Cosmochim. Acta* **68**, 3863 (2004).
23. M. Church, O. Slaymaker, *Nature* **337**, 452 (1989).
24. P. McLaren, T. Tuominen, in *Health of the Fraser River Aquatic Ecosystem, a Synthesis of Research Conducted under the Fraser River Action Plan, DOE FRAP 1998-11*, C. Colin, T. Tuominen, Eds. (Environment Canada, Vancouver, BC, Canada, 1999), vol. 1, chap. 3.4.
25. M. H. Conte, J. C. Weber, *Global Biogeochem. Cyc.* **16**, 10.1029/2002GB001922 (2002).
26. R. H. Smittenberg *et al.*, *Paleoceanography* **19**, 10.1029/2003PA000927 (2004).
27. D. J. Kovanen, D. J. Easterbrook, *Quat. Res.* **57**, 208 (2002).
28. J. W. Collister, É. Lichtfouse, G. Hieshima, J. M. Hayes, *Org. Geochem.* **21**, 645 (1994).
29. G. Gleixner, *et al.*, *Org. Geochem.* **33**, 357 (2002).
30. E. Lichtfouse *et al.*, *Geochim. Cosmochim. Acta* **61**, 1891 (1997).
31. S. Trumbore, *Ecol. Appl.* **10**, 339 (2000).
32. We thank the staff at the National Ocean Sciences Accelerator Mass Spectrometry Facility at Woods Hole, MA, USA, for help during preparation for ^{14}C analysis; M. Baas, M. Kienhuis (Royal Netherland Institute of Sea Research), and D. Montluçon (Woods Hole Oceanographic Institution) for assistance with the *n*-alkane isolation; The Ocean Drilling Project for providing subsamples obtained at leg 169S; and M. J. Whiticar (University of Victoria, Canada), for providing the pre- and post-bomb sediments. This research was primarily conducted by R.H.S., supported by a grant to J.S.S.D. from the Research Council for Earth and Life Science (ALW) with financial support from the Netherlands Organization for Scientific Research (NWO), and a grant to T.I.E. from NSF (OCE-0137005).

Recent Greenland Ice Mass Loss by Drainage System from Satellite Gravity Observations

S. B. Luthcke,[1]* H. J. Zwally,[2] W. Abdalati,[2] D. D. Rowlands,[1] R. D. Ray,[1] R. S. Nerem,[3] F. G. Lemoine,[1] J. J. McCarthy,[4] D. S. Chinn[4]

Mass changes of the Greenland Ice Sheet resolved by drainage system regions were derived from a local mass concentration analysis of NASA–Deutsches Zentrum für Luft- und Raumfahrt Gravity Recovery and Climate Experiment (GRACE mission) observations. From 2003 to 2005, the ice sheet lost 101 ± 16 gigaton/year, with a gain of 54 gigaton/year above 2000 meters and a loss of 155 gigaton/year at lower elevations. The lower elevations show a large seasonal cycle, with mass losses during summer melting followed by gains from fall through spring. The overall rate of loss reflects a considerable change in trend (−113 ± 17 gigaton/year) from a near balance during the 1990s but is smaller than some other recent estimates.

Mass changes in the Greenland Ice Sheet are of considerable interest because of its sensitivity to climate change and the potential for an increasing contribution of Greenland ice loss to rising sea level. Observations and models have shown that in recent years Greenland has experienced increased melt (*1*), thinning at the margins (*2–4*), and increased discharge from many outlet glaciers (*5*). At the same time, the ice sheet has been growing in its interior (*3*, *4*, *6*).

These recent changes in the Greenland Ice Sheet and the wide range of mass-balance estimates (*7*) highlight the importance of methods for directly observing variations in ice sheet mass. Moreover, the fact that some regions are shedding mass dramatically, whereas others are not (*2–5*), indicates a clear need for measurements with a spatial resolution that allows assessment of the behavior of individual drainage systems (DSs). The local mass concentration analysis presented here provides an assessment of mass balance of individual Greenland DS regions, subdivided by elevation, as well as the overall ice sheet mass balance.

Direct measurements of mass change have been enabled by the NASA–Deutsches Zentrum für Luft- und Raumfahrt Gravity Recovery and Climate Experiment (GRACE) mission (*8*). Since its launch in March 2002, GRACE has been acquiring ultra-precise (0.1 μm/s) intersatellite K-band range and range rate (KBRR) measurements taken between two satellites in polar orbit about 200 km apart. The changes in range rate sensed between these satellites provide a direct mapping of static and time-variable gravity.

Recent GRACE-based mass balance estimates of Antarctica (*9*) and Greenland (*10*, *11*) have been derived from the monthly spherical-harmonic gravity fields produced by the GRACE project. Although these solutions represent an important advance in the use of gravity measurements to assess ice sheet mass balance, they are limited in their temporal and spatial resolution. For example, the recent results presented in (*11*) showed sizable mass loss spread over the entire Greenland continent, in contrast with recent studies that indicated loss concentrated on the margins (*2–5*) and growth in the interior (*3*, *4*, *6*). In addition, the fundamental measurements being made by GRACE contain far more information than is currently being exploited by techniques that rely on these monthly

[1]Planetary Geodynamics Laboratory, Code 698, NASA Goddard Space Flight Center, Greenbelt, MD 20771, USA. [2]Cryospheric Sciences Branch, Code 614.1, NASA Goddard Space Flight Center, Greenbelt, MD 20771, USA. [3]Colorado Center for Astrodynamics Research, Cooperative Institute for Research in Environmental Sciences, Department of Aerospace Engineering Sciences, University of Colorado, Boulder, CO 80309, USA. [4]Science Division, SGT Incorporated, Greenbelt, MD 20770, USA.

*To whom correspondence should be addressed. E-mail: Scott.B.Luthcke@nasa.gov